

High-power (>10 W) continuous-wave operation from 100- μm -aperture 0.97- μm -emitting Al-free diode lasers

A. Al-Muhanna,^{a)} L. J. Mawst, and D. Botez

Reed Center for Photonics, Electrical and Computer Engineering Department, University of Wisconsin–Madison, Madison, Wisconsin 53706

D. Z. Garbuzov, R. U. Martinelli, and J. C. Connolly

Sarnoff Corporation, 201 Washington Road, Princeton, New Jersey 08543

(Received 11 February 1998; accepted for publication 1 July 1998)

By incorporating a broad transverse waveguide (1.3 μm) in 0.97- μm -emitting InGaAs(P)/InGaP/GaAs separate-confinement-heterostructure quantum-well diode-laser structures we obtain record-high continuous-wave (cw) output powers for any type of InGaAs-active diode lasers: 10.6–11.0 W from 100- μm -wide-aperture devices at 10 °C heatsink temperature, mounted on either diamond or Cu heatsinks. Built-in discrimination against the second-order transverse mode allows pure fundamental-transverse-mode operation ($\theta_{\perp} = 36^{\circ}$) to at least 20-W-peak pulsed power, at $68\times$ threshold. The internal optical power density at catastrophic optical mirror damage (COMD) \bar{P}_{COMD} is found to be 18–18.5 MW/cm² for these conventionally facet-passivated diodes. The lasers are 2-mm-long with 5%/95% reflectivity for front/back facet coating. A low internal loss coefficient ($\alpha_i = 1 \text{ cm}^{-1}$) allows for high external differential quantum efficiency η_d (85%). The characteristic temperatures for the threshold current T_0 and the differential quantum efficiency T_1 are 210 and 1800 K, respectively. Low differential series resistance R_s : 26 m Ω ; leads to electrical-to-optical power conversion efficiencies in excess of 40% from 1 W up to 10.6 W cw output power, and as much as 50% higher than those of 0.97- μm -emitting Al-containing devices. © 1998 American Institute of Physics. [S0003-6951(98)03335-X]

Broad-stripe, InGaAs-active diode lasers ($\lambda = 0.89\text{--}1.06 \mu\text{m}$) are routinely used for pumping solid-state fiber lasers, frequency doubling, and for numerous medical applications. Al-free devices (i.e., InGaAs/InGaP/GaAs structures) have superior “wallplug” efficiency compared with conventional Al-containing devices¹ due to their low differential series resistance.^{1,2} Furthermore, the low oxidation rate of InGaP permits high-quality epitaxial regrowths over gratings for longitudinal-mode control (i.e., distributed-feedback lasers)^{3,4} or over etched structures for lateral-mode control.^{5–9} Thus, the Al-free material system is highly desirable for both broad-stripe spatially incoherent devices as well as for temporally and/or spatially coherent index-guided diode lasers.

Recently, we have reported¹⁰ continuous-wave (cw) output powers of 8 W from 0.98- μm -emitting InGaAs/InGaP/GaP lasers of a 100- μm -wide stripe, 4-mm-long cavity, 1- μm -thick transverse waveguide, and mounted on Cu heatsinks. Such broad-waveguide (BW) devices also demonstrated fundamental-transverse-mode operation to high drive levels,¹¹ as expected since the cutoff thickness for the second-order transverse mode is 1.05 μm . BW devices with a waveguide thickness of 1.3 μm exhibited lasing in both the fundamental and the second-order transverse modes.¹²

We report here maximum cw output powers of 10.6–11 W, record-high values for any type of InGaAs-active-region diode lasers. The devices show pure fundamental-transverse-mode operation to at least 20 W peak pulsed power. We

achieve these results using a 1.3- μm -waveguide structure, designed to suppress oscillation of the second-order transverse mode.

The InGaAs(P)/InGaP/GaAs laser structure used is shown in Fig. 1. It was grown by low-pressure metal-organic chemical vapor deposition in an Aixtron A-200 system on exact-oriented (100) GaAs substrates.¹³ The structure

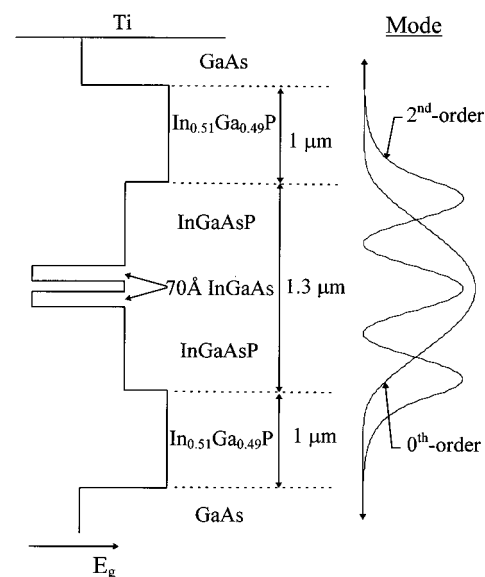


FIG. 1. Schematic representation of Al-free, broad-waveguide 0.97- μm -emitting diode laser. The field intensity profiles for the fundamental- and second-order transverse modes are shown on the right side. The first-order transverse mode is not shown since it has negligible field overlap Γ with the active region (i.e., the two quantum wells).

^{a)}Electronic mail: al-muhan@cae.wisc.edu

consists of two 70-Å-thick $\text{In}_{0.2}\text{Ga}_{0.8}\text{As}$ quantum wells, a 1.3- μm -thick InGaAsP ($E_g = 1.6$ eV) waveguide region, 1.0- μm -thick $\text{In}_{0.51}\text{Ga}_{0.49}\text{P}$ cladding layers, and a 0.2- μm -thick p^+ -GaAs cap layer.

Fabry-Perot lasers with 100- μm -wide metal contact stripes were fabricated by using conventional oxide-defined window-stripe processing. The p - and n -side metal contacts were Ti/Pt/Au and Ge/AuGe/Ni/Au, respectively. The lasing wavelength was 0.97 μm at 15 °C.

The structures used here are similar to previous structures,^{10–12} except for a notable difference in the thickness of the InGaP cladding layers: it has been reduced from 1.5 to 1.0 μm . This reduction has no effect on the fundamental mode. The first-order mode cannot lase since it has negligible (transverse) optical field overlap Γ with the quantum wells. The second-order mode, however, is strongly influenced by thinning the cladding layers. That is, the second-order mode suffers both (transverse) radiation losses to the substrate as well as absorption loss in the p -side metal contact. The first layer in the p -side metal contact, Ti, has a refractive index at $\lambda = 0.98$ μm (i.e., $n = 3.3 + i.3.26$), which gives a light penetration depth of 240 Å (i.e., only 60% of its actual thickness), and thus, can be considered semi-infinite. The second-order mode loss is then found to increase from 2.2 to 37.4 cm^{-1} as the cladding layers' thickness decreases from 1.5 to 1.0 μm . In turn, using an experimentally determined¹ logarithmic gain versus threshold-current density J_{th} relationship, with 2.1% and 1.35% values for the Γ 's of the fundamental and second-order mode, respectively, we estimate that the second-order mode has a J_{th} value 11.8 times that for the fundamental mode. As a result, the device operates in the fundamental transverse mode [Fig. 2(a)] to 20-W-peak pulsed power (0.5- μs -wide pulses, 200-Hz repetition rate) at a drive current of 27 A (i.e., $68 \times$ threshold) in a virtual Gaussian beam pattern ($\theta_{\perp,1/2} = 36^\circ$, $\theta_{\perp,1/e^2} = 62.5^\circ$) identical to that predicted by theory [Fig. 2(b)]. (The peak output power was limited by the maximum drive current of our power supply.)

It should be noted that for 1.5- μm -thick cladding layers the J_{th} of the second-order mode is only 1.6 times higher than that for the fundamental mode, solely based on the different Γ values for the two modes. Since in broad-stripe devices uniform lasing does not occur over the whole aperture until the drive current reaches ~ 2 times the threshold current, it is quite likely that at $1.6 J_{\text{th}}$ unused gain is available for lasing to start in the second-order transverse mode. As a result, one obtains in the far field a combination of the fundamental and second-order transverse modes,¹² as shown by the dashed curve in Fig. 2(b). For the case shown in Fig. 2(b) the beamwidth at $1/e^2$ points in intensity is 20% larger than theory predicts, which can be easily shown to mean that $\sim 16\%$ of the energy is emitted in the second-order mode. (The $\theta_{1/2}$ value is virtually unaffected, since the second-order-mode beam pattern has intensity nulls at $\pm 16.5^\circ$.)

The use of a broad-waveguide structure results in an optical-field distribution almost entirely confined to the nominally undoped waveguide region. As a result, a low internal loss coefficient $\alpha_i = 1$ cm^{-1} is obtained, which in turn provides a relatively high value for the external differential quantum efficiency $\eta_d = 85\%$ for 2-mm-long, 5%/95%
Downloaded 20 Dec 2006 to 128.104.198.71. Redistribution subject to AIP license or copyright, see http://apl.aip.org/apl/copyright.jsp

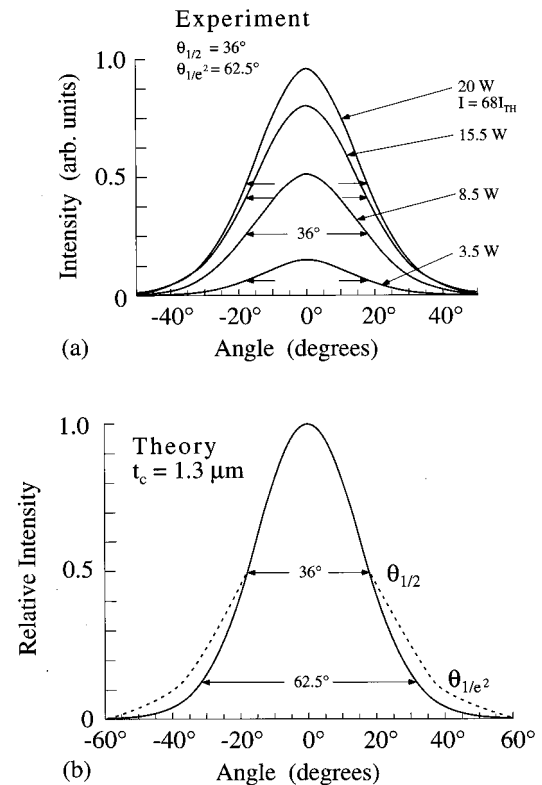


FIG. 2. (a) Transverse far-field patterns at various peak output powers in pulsed operation (0.5 μs pulse width, 200 Hz repetition rate) for the device shown in Fig. 1. I_{th} is the threshold current and has a value of 0.4 A for 100 $\mu\text{m} \times 2$ mm contact devices. (b) Theoretical far-field pattern for the device shown in Fig. 1 and typical experimental far-field pattern for 1.5- μm -thick cladding-layer devices (Ref. 12) (dashed curve).

coated devices. High cw output powers are attained by taking advantage of the relatively large equivalent transverse spot size,¹⁰ d/Γ : 0.66 μm ; where d is the quantum-well(s) thickness. Cw output power as high as 10.6 W [Fig. 3(a)] is achieved from 2-mm-long, 100- μm -wide aperture devices at 10 °C heatsink temperature and mounted on diamond submounts. Two other devices reached 10.5 and 10 W cw output power. The internal optical power density at catastrophic optical-mirror damage (COMD),¹⁰ \bar{P}_{COMD} , is ≈ 18 MW/ cm^2 , a value quite similar to the 19 MW/ cm^2 obtained¹⁵ from InGaAs/AlGaAs high-power devices mounted on Cu heat-sinks; proving that when the maximum cw power is limited by COMD (rather than due to thermal considerations), the chip thermal resistance is low due to large contact area, and η_d is relatively temperature insensitive (i.e. high T_1 values),¹³ the use of diamond or Cu heatsinks makes no difference. More recently, we obtained¹⁴ 11 W cw at 10 °C, from identical devices mounted on Cu heatsinks, thus further confirming the above conclusion. The 10.6–11.0 W cw power levels are, to the best of our knowledge, the highest cw powers reported from any type of semiconductor lasers with an InGaAs active region.

The threshold-current density J_{th} and the differential quantum efficiency η_d were measured in pulsed operation as the heatsink temperature was varied from 20 to 80 °C. A best-fit analysis gives characteristic temperatures for the threshold current T_0 and the external differential quantum efficiency¹³ T_1 of 210 and 1800 K, respectively. That is, η_d

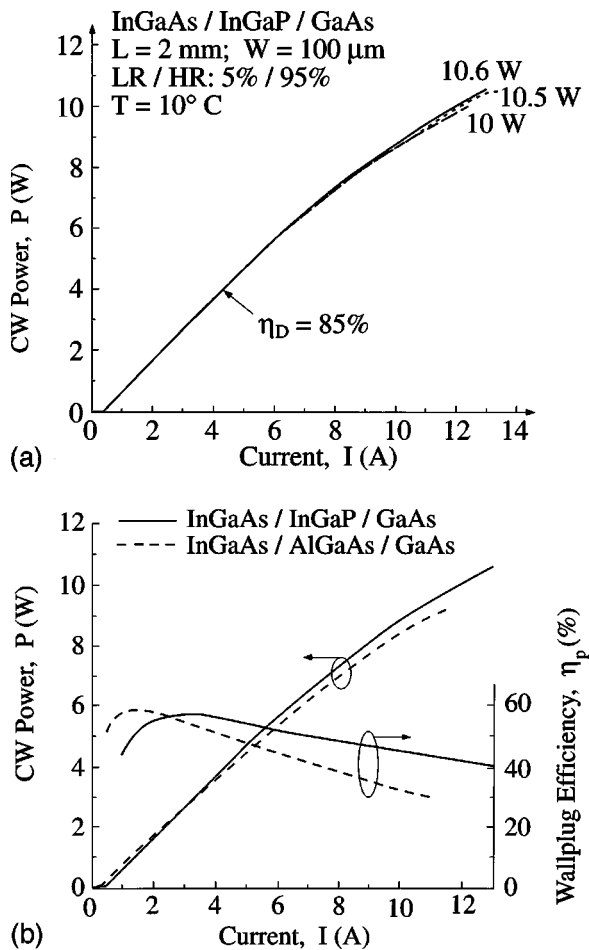


FIG. 3. (a) Cw light-current characteristics for three typical 0.97- μm -emitting diodes at 10 $^{\circ}\text{C}$ heatsink temperature. (b) Cw light-current characteristics and "wallplug" efficiency curves at 10 $^{\circ}\text{C}$ for 100- μm -stripe, 2-mm-long, 0.97- μm -emitting lasers. Solid lines: Al-free structure shown in Fig. 1. Dashed lines: InGaAs/AlGaAs/GaAs device (Ref. 15).

decreases by only 3% between 20 and 80 $^{\circ}\text{C}$. The relatively high values obtained for T_0 and T_1 reflect excellent carrier confinement. By comparison, the T_0 and T_1 values for 0.97- μm -emitting, high-power AlGaAs-cladding devices¹⁵ of the same dimensions are significantly lower: 150 and 760 K, respectively; even though the temperature range is narrower (15–60 $^{\circ}\text{C}$).

A comparison to 0.97- μm -emitting InGaAs/AlGaAs devices of the same geometry and driven under the same conditions: cw and 10 $^{\circ}\text{C}$ heatsink temperature; is shown in Fig. 3(b). The difference in maximum cw power simply reflects the smaller d/Γ value (i.e., 0.53 μm)¹⁵ for the Al-containing devices. The most relevant and significant difference is in "wallplug" efficiency, η_p , due to the fact that InGaP-cladded devices have a series resistance $R_s = 26\text{--}28$ m Ω , about four times less than R_s values for the 0.97- μm -

emitting, AlGaAs-cladded devices of the same contact geometry.¹⁵ Although η_p reaches basically the same maximum value for both structures, for Al-free devices η_p is higher and decreases much more slowly with increasing drive current than it does for Al-containing devices. Thus, at the 9 W cw power level, η_p of Al-free devices is 50% higher (i.e., 45% versus 30%) than η_p of Al-containing devices. Higher wallplug efficiency coupled with significantly less Joule heating should permit Al-free devices to operate reliably at higher cw powers than Al-containing devices.

In conclusion, we report on 0.97- μm -emitting Al-free lasers with record-high cw output powers, 10.6–11.0 W, for InGaAs-active devices; low internal loss, $\alpha_i = 1$ cm^{-1} ; and high characteristic temperatures, $T_0 = 210$ K, $T_1 = 1800$ K. Furthermore, built-in discrimination against the second-order transverse mode allows stable fundamental-transverse-mode operation to 20-W-peak pulsed power.

The authors gratefully acknowledge support by the Air Force Phillips Laboratory, under Contract No. F29601-96-C-0140, and the National Science Foundation, Grant No. BES-9612244; as well as the valuable technical assistance of J. A. Morris and technical discussions with P. Zory.

- ¹D. Botez, L. J. Mawst, A. Bhattacharya, J. Lopez, J. Li, T. F. Kuech, V. P. Iakovlev, G. I. Suruceanu, A. Caliman, and A. V. Syrbu, *Electron. Lett.* **32**, 2012 (1996).
- ²A. Al-Muhanna, L. J. Mawst, D. Botez, D. Z. Garbuzov, R. U. Martinelli, and J. Connolly, *Appl. Phys. Lett.* **71**, 1142 (1997).
- ³Y. K. Sin and M. Horikawa, *Electron. Lett.* **29**, 240 (1993).
- ⁴M. Nesnidal, T. Earles, L. J. Mawst, D. Botez, and J. Buus, *Appl. Phys. Lett.* **73**, 587 (1998).
- ⁵S. H. Groves, Z. L. Liao, S. C. Palmateer, and J. N. Walpole, *Appl. Phys. Lett.* **56**, 312 (1990).
- ⁶E. C. Vail, S. F. Lim, Y. A. Wu, D. A. Francis, C. J. Chang-Hasnain, R. Bhat, and C. Caneau, *Appl. Phys. Lett.* **63**, 2183 (1993).
- ⁷M. Sagawa, T. Toyonaka, K. Hiramoto, K. Shinoda, and K. Uomi, *IEEE J. Sel. Top. Quantum Electron.* **1**, 189 (1995).
- ⁸A. Bhattacharya, L. J. Mawst, M. Nesnidal, J. Lopez, and D. Botez, *Electron. Lett.* **32**, 657 (1996).
- ⁹H. Yang, L. J. Mawst, M. Nesnidal, J. Lopez, A. Bhattacharya, and D. Botez, *Electron. Lett.* **33**, 136 (1997).
- ¹⁰L. J. Mawst, A. Bhattacharya, J. Lopez, D. Botez, D. Z. Garbuzov, L. DeMarco, J. C. Connolly, M. Jansen, F. Fang, and R. F. Nabiev, *Appl. Phys. Lett.* **69**, 1532 (1996).
- ¹¹D. Garbuzov, N. Morris, B. Odubango, R. Martinelli, J. C. Connolly, L. J. Mawst, A. Bhattacharya, D. Botez, C. Dries, and S. R. Forrest, *Tech. Dig. IEEE/OSA Conference on Lasers and Electro-Optics '97*, Baltimore, MD; **11**, 3 (1997).
- ¹²D. Garbuzov and J. C. Connolly (unpublished).
- ¹³L. J. Mawst, A. Bhattacharya, M. Nesnidal, J. Lopez, D. Botez, J. Morris, and P. Zory, *Appl. Phys. Lett.* **67**, 2901 (1995).
- ¹⁴D. Z. Garbuzov, M. G. Harvey, J. C. Connolly, M. A. Maiorov, A. Al-Muhanna, L. Mawst, and D. Botez (unpublished); and D. Z. Garbuzov, *Tech. Dig. IEEE/OSA Conference on Lasers and Electro-Optics '98*, San Francisco, CA, (1998), Vol. 6, p. 10.
- ¹⁵S. O'Brien, H. Zhao, A. Schoenfelder, and R. J. Lang, *Electron. Lett.* **33**, 1869 (1997).